Galaxies, Cosmology and Dark Matter

Lecture given by
Ralf Bender
USM

Script by:
Christine Botzler, Armin Gabasch,
Georg Feulner, Jan Snigula

Summer semester 2000

Chapter 5

Spiral Galaxies

5.8 Rotation of Spirals

5.8.1 Rotational Properties of Exponential Disks

Apart from the central bulge, most of the stars in spirals are concentrated in a relatively thin disk. How does the rotation curve of a thin exponential disk look like?

Outside the disk we have to solve the **Laplace equation** (in cylindrical coordinates):

$$\frac{1}{R}\frac{\partial}{\partial R}\left(R\frac{\partial \Phi}{\partial R}\right)+\frac{\partial^2 \Phi}{\partial z^2}=0$$

By separation of variables:

$$\Phi = I(R)Z(z)$$

we get:

$$\frac{1}{I(R)R}\frac{d}{dR}\left(R\frac{dI}{dR}\right)=-\frac{1}{Z(z)}\frac{d^2Z}{dz^2}=-k^2$$

with a constant k. These two differential equations are solved by:

$$Z(z) = Z_0 e^{-k|z|} \quad Z_0 = \text{ const.}$$
$$I(R) = I_0(kR)$$

with $I_0(kR)$ being the cylindrical Bessel function of 0th order. The boundary conditions are chosen such that $\Phi \to 0$ for $z \to \infty$ or $R \to \infty$ and $\Phi(z = 0)$ remains finite.

Consequently:

$$\Phi_k(R, z) = Z_0 e^{-k|z|} I_0(kR)$$

is the solution of $\vec{\nabla}^2 \Phi = 0$ outside of an infinitely thin, finite axially symmetric mass distribution.

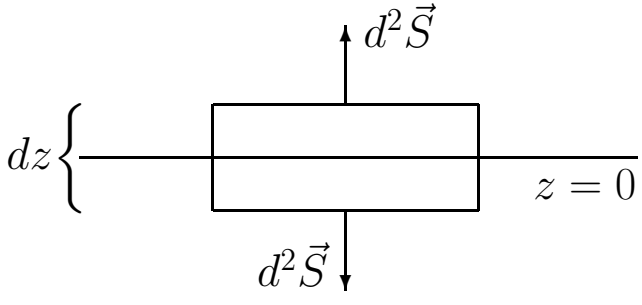

$\Phi_k(R,z)$ is valid everywhere except at $z=0$, because of the discontinuity of $\vec{\nabla}\Phi_k$ at this surface. The mass surface density Σ corresponding to this discontinuity can be determined from **Gauss's theorem**:

$$\int \vec{\nabla}^2\Phi_k d^3x = 4\pi G \int \rho d^3x$$

$$\rightsquigarrow \int \vec{\nabla}\Phi_k d^2S = 4\pi G \int \underbrace{\left(\int \rho dz\right)} d^2S$$

$$\left(\begin{array}{c}\text{contribution of}\\ \text{other surface elements}\\ \rightarrow 0 \text{ for } d^3x \rightarrow 0\end{array}\right) \rightsquigarrow \left(\frac{\partial\Phi_+}{\partial z} - \frac{\partial\Phi_-}{\partial z}\right) d^2S = 4\pi G\Sigma_k d^2S$$

with Σ_k the mass surface density, and:

$$\frac{\partial\Phi_\pm}{\partial z} = \lim_{z\rightarrow 0^+_-} \frac{\partial\Phi_k}{\partial z} = \mp\, kI_0(kR)$$

The surface density corresponding to the solution $\Phi_k(z,R)$ therefore is:

$$\Sigma_k(R) = -\frac{k}{2\pi G} I_0(kR)$$

Due to the linearity of **Poisson's equation** in Φ and ρ, we can use superposition to obtain more general solutions:

$$\Sigma(R) = \int_0^\infty S(k)\Sigma_k(R)dk$$

and

$$\Phi(R,z) = \int_0^\infty S(k)\Phi_k(R,z)dk$$

to derive the potential of an arbitrary very thin density distribution. If $\Sigma(R)$ is given, we have to invert:

$$\Sigma(R) = -\frac{1}{2\pi G}\int_0^\infty S(k)I_0(kR)kdk$$

The integral equals a Hankel transformation, with its inversion given by:

$$S(k) = -2\pi G\int_0^\infty I_0(kR)\Sigma(R)RdR$$

Setting

$$\Sigma(R) = \Sigma_0 e^{-\frac{R}{R_0}},$$

we can deduce Φ and $v_c^2 = R\frac{\partial \Phi}{\partial R}$ of the exponential disk (I_0, I_1, K_0, K_1 are modified Bessel functions):

$$R\frac{\partial \Phi}{\partial R} = \boxed{v_c^2(R) = 4\pi G \Sigma_0 R_0 y^2 \left(I_0(y)K_0(y) - I_1(y)K_1(y)\right)}$$

with $y = \frac{1}{2}\frac{R}{R_0}$ and, as usual: $\Sigma(R) = \Sigma(0)e^{-\frac{R}{R_0}}$

Approximation: $v_c \simeq 0.876\sqrt{\frac{GM}{R_0}} \cdot \sqrt{\frac{\tilde{r}^{1.3}}{1+\tilde{r}^{2.3}}}$ (for $R < 4R_0$)

with $\tilde{r} = 0.533\frac{R}{R_0}$

Maximum at $R_{\text{max}} \simeq 2.2R_0$
Kepler fall-off at $R_{\text{Kepler}} \gtrapprox 3R_{\text{max}}$

Rotation curve of the thin exponential disk:

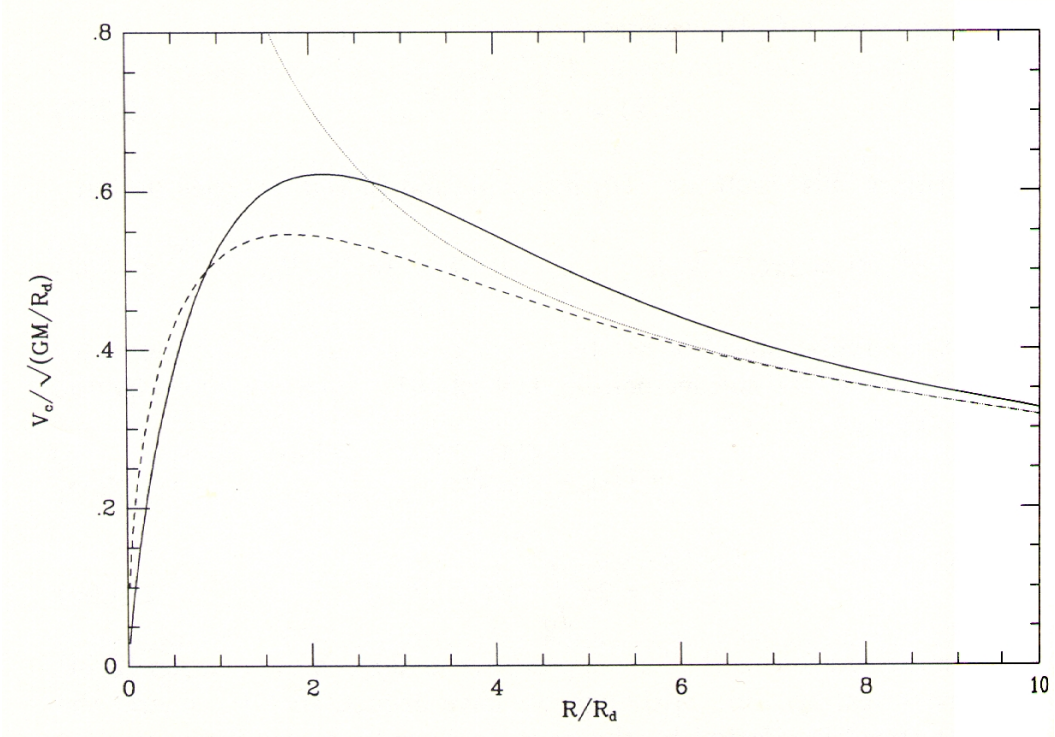

Figure 2-17. The circular-speed curves of: an exponential disk (full curve); a point with the same total mass (dotted curve); the spherical body for which $M(r)$ is given by equation (2-170) (dashed curve).

see: Binney, Tremaine (1994) *Galactic Dynamics*, p. 78

5.8.2 Experimental Determination of the Rotation of Spiral Galaxies

- The **circular speed** can be approximately determined as a function of the radius by measuring the **redshift of the emission lines** of the gas contained in the disk.
  - hot stars ionize gas:
    $\Rightarrow$ **hydrogen emission lines**, mainly **H**$_\alpha$ in the optical.
  - neutral atomic hydrogen gas:
    hyperfine structure transition ($\uparrow_p\uparrow_e \rightarrow \uparrow_p\downarrow_e$) leads to a **21cm radio line**. (population of the $\uparrow\uparrow$ state by radiation or electron collisions)
- The **dynamical mass** of a spiral galaxy within the radius r is:

$$\boxed{M(<r) = \frac{\alpha}{G} r v_{rot}^2(r)}$$

α is a geometry factor. For the same radial density distribution but different flattenings (disk vs. sphere) one has $0.8 < \alpha < 1.2$.

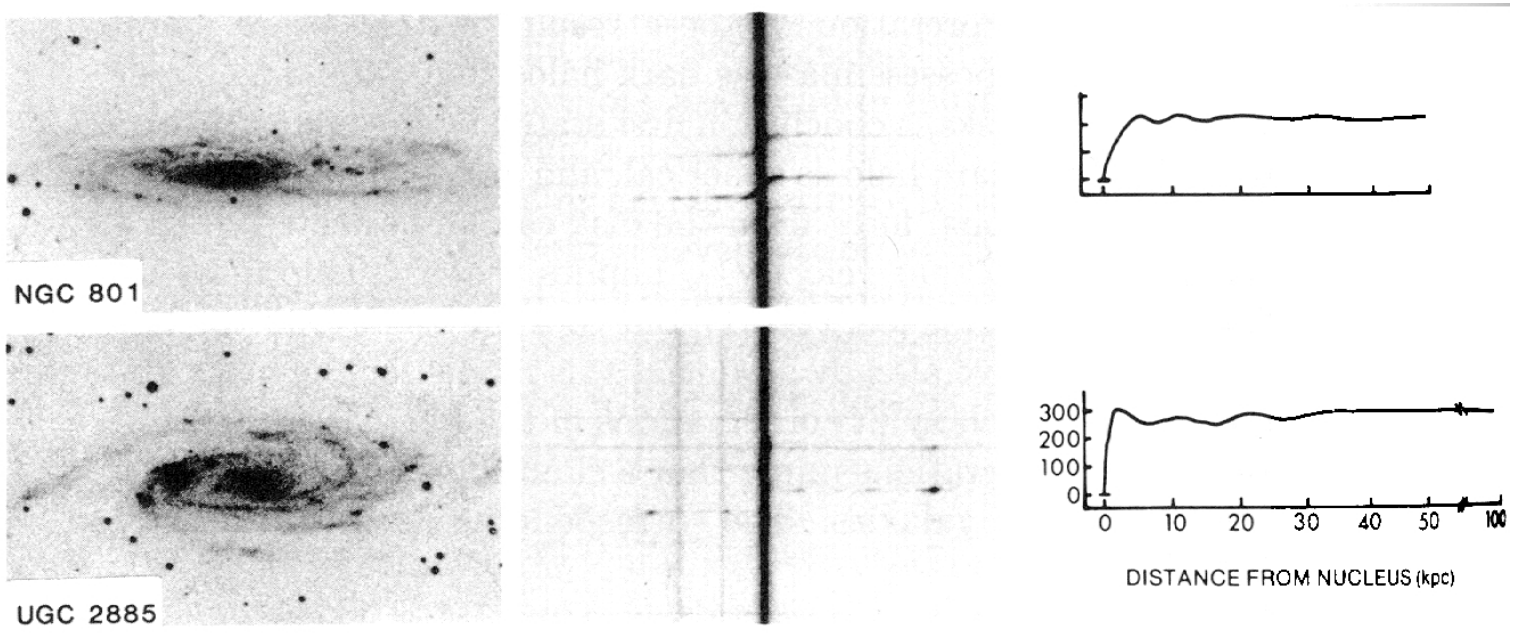

Figure 10-1. Photographs, spectra, and rotation curves for five Sc galaxies, arranged in order of increasing luminosity from top to bottom. The top three images are television pictures, in which the spectrograph slit appears as a dark line crossing the center of the galaxy. The vertical line in each spectrum is continuum emission from the nucleus. The distance scales are based on a Hubble constant $h = 0.5$. Reproduced from Rubin (1983), by permission of *Science*.

see: Binney, Tremaine (1994) *Galactic Dynamics* p.600

HI-rotation curves of spiral galaxies:

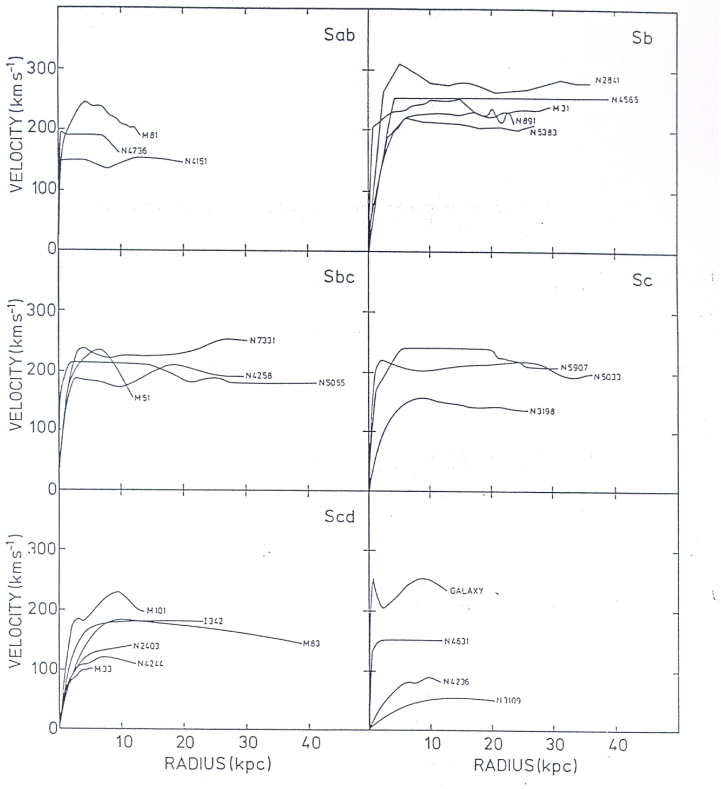

FIGURE 1. Rotation curves of 25 galaxies of various Hubble types.

see: Bosma (1979) *PhD Thesis*

Rotation Curve of the Galaxy:

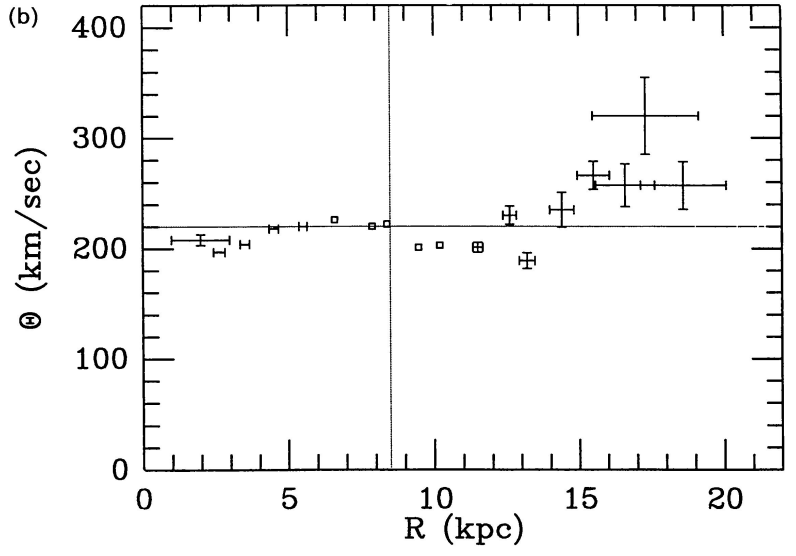

Figure 2 The rotation curve of the Galaxy for the 1985 IAU values $R_o = 8.5$ kpc, $\Theta_o = 220$ km s^{-1} (*dotted lines*). (*a*) Individual data points and associated error bars. Open squares: planetary nebulae from Schneider & Terzian (1983); open circles: CO tangent points from Clemens (1985); open triangles: H II regions from Chini & Wink (1985); stars: open clusters from Hron (1987); asterisks: H I tangent points from Burton & Gordon (1978); naked error bars: H II regions from Fich et al (1989). (*b*) Averaged rotation curve using data in (*a*). The error bars are plotted using the overly optimistic assumption that errors in R and Θ, as well as errors in different data points, are all Gaussian and uncorrelated. Open squares denote cases in which the error bar is smaller than the size of the symbol. Errors in distances determined by the tangent point method are taken to be 1 kpc.

see: Fich et al. (1991) *ARAA*, **29**, 409

5.8.3 The Tully-Fisher Relation

- Relation between circular speed v_{circ} and luminosity of spiral galaxies:

$$L \sim v_{circ}^{3...4}$$

(The power depends on the wavelength of L, because of changing M/L, star formation, etc.)

- From the virial theorem, $v_{circ}^2 \sim \frac{M}{r}$, and the identity $L \sim \Sigma r^2$ (with Σ: surface brightness) one obtains:

$$L \sim \left(\frac{M}{L}\right)^{-2} v_{circ}^4 \Sigma^{-1}$$

Evidently the observed Tully-Fisher relation implies: $\left(\frac{M}{L}\right)^{-2} \cdot \Sigma^{-1} \simeq \mathrm{const}$. Indeed, most bright spirals have similar mass-to-light ratios and surface brightnesses: $\frac{M}{L} \sim \mathrm{const}$ and $\Sigma \sim \mathrm{const}$ (the latter is called the “Freeman law”).

- The Tully-Fisher relation is of fundamental importance for the distance determination of spiral galaxies.

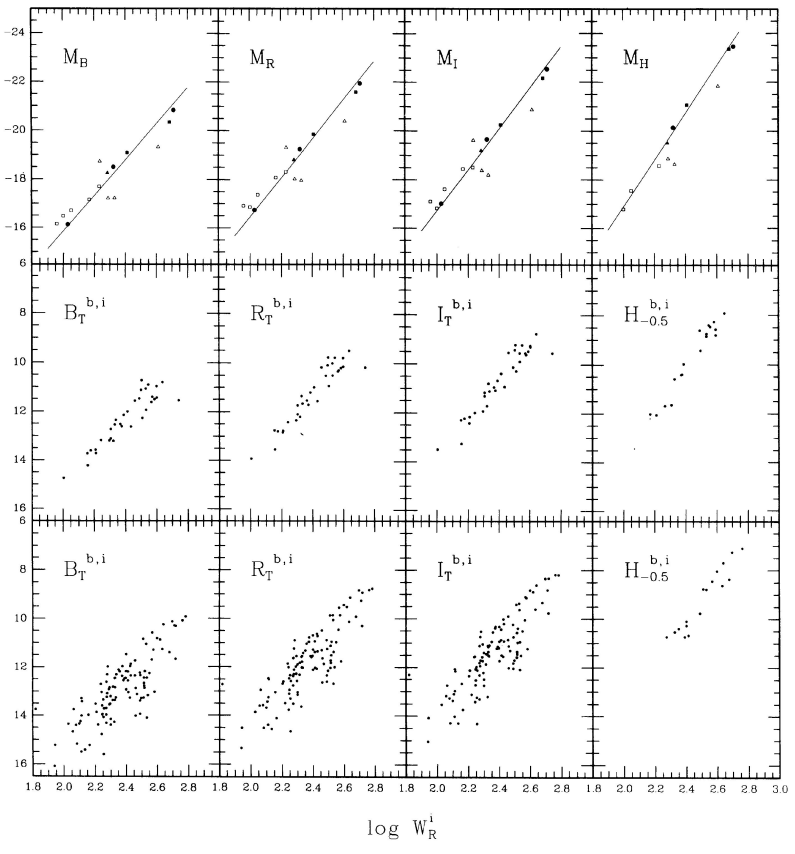

FIG. 11—*B*-, *R*-, *I*-, and *H*-band Tully–Fisher relations for the Local Calibrators (top), Ursa Major cluster members (middle), and Virgo cluster members (bottom). It is apparent from the figures that the slope of the relations increases going to longer wavelengths and the dispersion decreases. The variation in slope is thought to arise from the differing contributions to the observed bandpass made by greater fraction of young stars found in the lower-luminosity systems. The smaller dispersion at longer wavelengths is likely due to a reduction in the sensitivity to these effects, as well as those expected from extinction variations. Note the much larger dispersion found for the Virgo cluster data.

see: Jacoby et al. (1992) *PASP*, **104**, 599

$W_R^i = 2v_{circ}$
v_{circ} can be deduced from HI observations;
correction for inclination adopting flattening of optical image.

5.9 Dark Matter in Spiral Galaxies

5.9.1 Dark Matter from Rotation Curves

Important paper:

DISTRIBUTION OF DARK MATTER IN THE SPIRAL GALAXY NGC 3198

T. S. VAN ALBADA,[1] J. N. BAHCALL,[2] K. BEGEMAN,[1] AND R. SANSCISI[1]

Received 1984 August 13; accepted 1985 February 26

ABSTRACT

Two-component mass models, consisting of an exponential disk and a spherical halo, are constructed to fit a newly determined rotation curve of NGC 3198 that extends to 11 disk scale lengths. The amount of dark matter inside the last point of the rotation curve, at 30 kpc, is at least 4 times larger than the amount of visible matter, with $(M/L_B)_{\rm tot} = 18\ M_\odot/L_{B\odot}$. The maximum mass-to-light ratio for the disk is $M/L_B = 3.6$. The available data cannot discriminate between disk models with low M/L and high M/L, but we present arguments which suggest that the true mass-to-light ratio of the disk is close to the maximum computed value. The core radius of the distribution of dark matter is found to satisfy $1.7 < R_{\rm core} < 12.5$ kpc.

Subject headings: galaxies: individual — galaxies: internal motions — interstellar: matter

see: van Albada et al. (1985) *ApJ*, **295**, 305

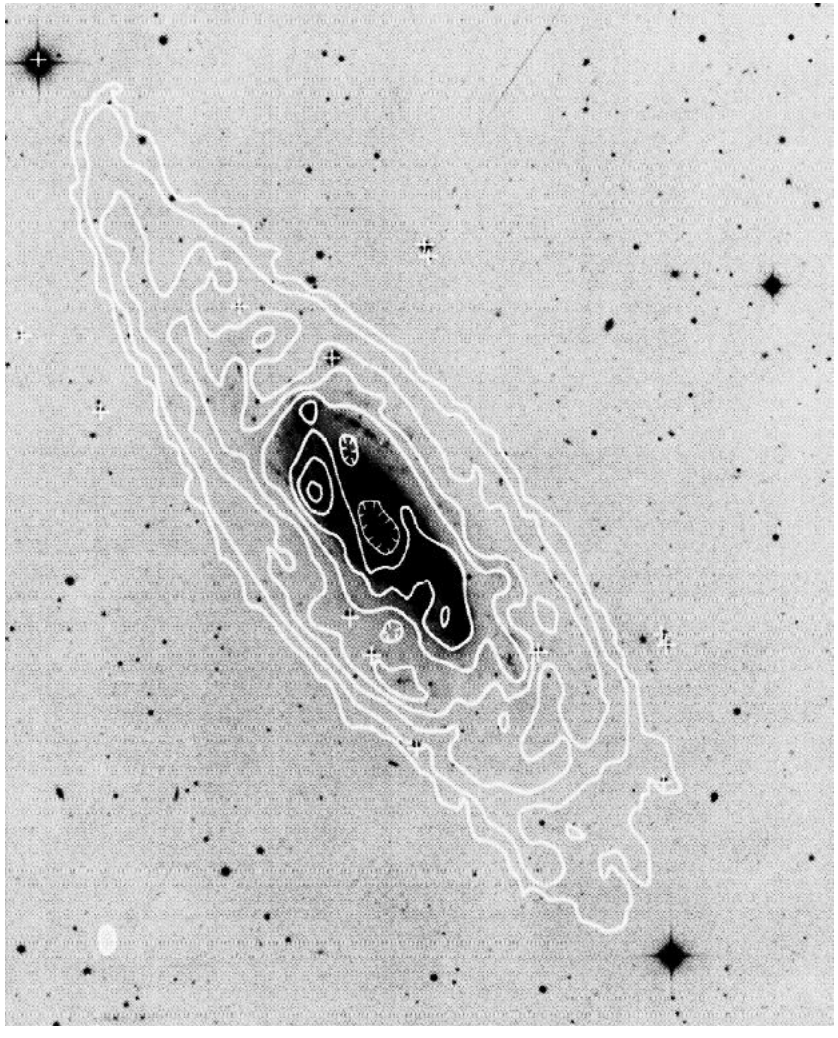

NGC 3198 (optical and radio emission)
HI measured using 21cm transition

see: van Albada et al. (1985) *ApJ*, **295**, 305

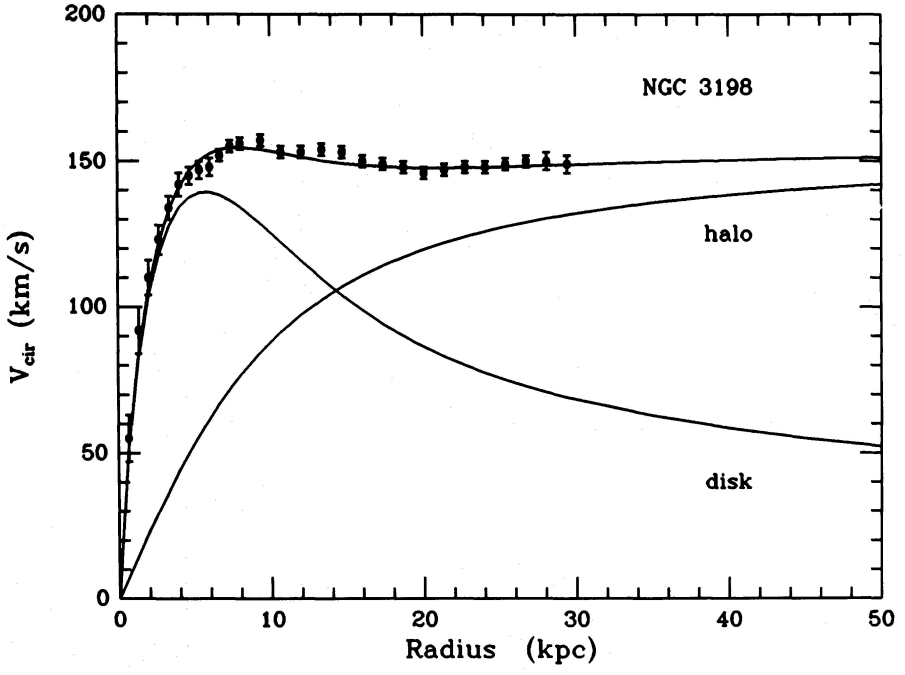

FIG. 4.—Fit of exponential disk with maximum mass and halo to observed rotation curve (*dots with error bars*). The scale length of the disk has been taken equal to that of the light distribution (60″, corresponding to 2.68 kpc). The halo curve is based on eq. (1), $a = 8.5$ kpc, $\gamma = 2.1$, $\rho(R_0) = 0.0040\ M_\odot\ \mathrm{pc}^{-3}$.

see: van Albada et al. (1985) *ApJ*, **295**, 305

$$\Phi = \Phi_{halo} + \Phi_{disc} \Rightarrow v_{circ}^2 = v_{c,halo}^2 + v_{c,disc}^2 \left(v_{circ}^2 = r\frac{\partial \Phi}{\partial r} \right)$$

Simple Model for Dark Matter Haloes:

Assume: $\rho = \rho_0 \dfrac{a^2}{r^2 + a^2} \qquad \left(r \gg a \rightarrow \rho \sim r^{-2}\right)$

$$M(r) = \int_0^r 4\pi\rho r^2 dr \qquad \text{(Bronstein No. 65)}$$

$$= 4\pi\rho_0 a^3 \left(\frac{r}{a} - \arctan\frac{r}{a}\right)$$

circular velocity (from virial theorem): $v_{circ}(r) = \sqrt{\dfrac{GM(r)}{r}}$

$$v_{circ}(r) = \left[4\pi G\rho_0 a^2 \left(1 - \frac{a}{r}\arctan\frac{r}{a}\right)\right]^{\frac{1}{2}}$$

$$r \gg a: \quad v_{circ} \rightarrow \sqrt{4\pi G\rho_0 a^2} \simeq \text{const}$$

$$r \ll a: \quad v_{circ} \rightarrow \sqrt{\frac{4\pi G\rho_0 a^2}{3}} \cdot \frac{r}{a}$$

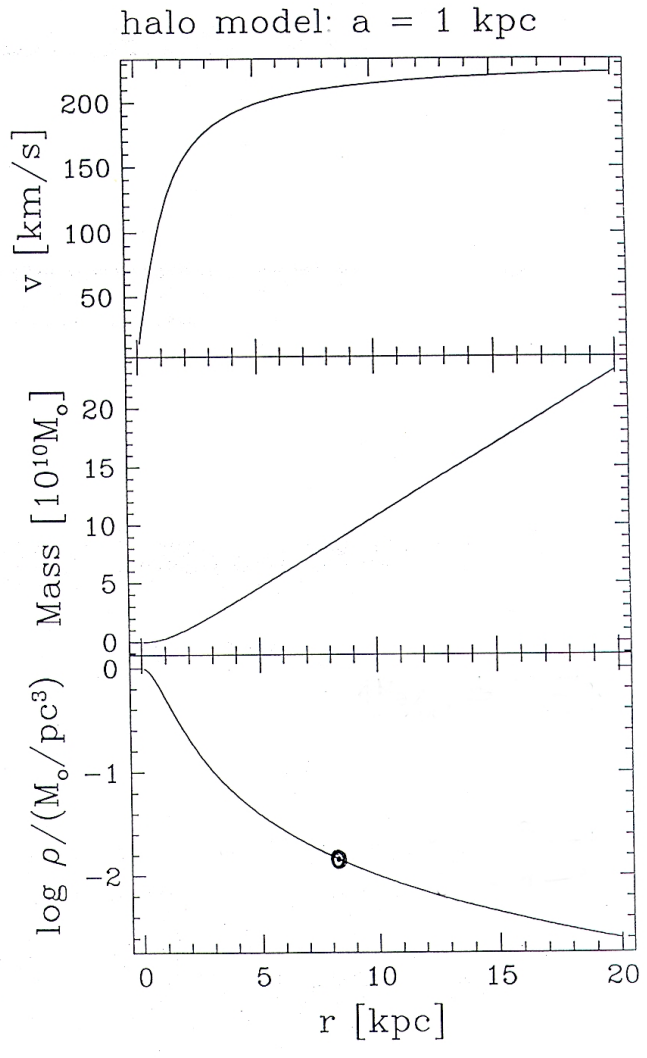
halo model: a = 1 kpc
v [km/s]
200
150
100
50
Mass [$10^{10}M_\odot$]
20
15
10
5
0
log $\rho/(M_\odot/pc^3)$
0
−1
−2
0
5
10
15
20
r [kpc]

Summary on Rotation Curves and Dark Matter:

Main observational fact:

Rotation curves remain flat out to radii much larger than the extent of the optical disk!

- From $v_{circ}(R) \simeq$ constant and centrifugal equilibrium $\frac{GM(R)}{R^2} = \frac{v_{circ}^2}{R}$, it follows:

$$M(R) \sim R \quad \text{(divergent!)}$$

- For the majority of spiral galaxies no decrease in the circular velocity has been measured even beyond radii of 50 kpc to 100 kpc.

$$\Rightarrow \boxed{\frac{M}{L_B} \gtrsim 30 \frac{M_\odot}{L_{B,\odot}} \quad \text{for spirals}}$$

$\frac{M}{L_B}$ of the observable matter in the galactic disk only:

$$\boxed{\frac{M}{L_B}(\text{stars and gas}) \simeq 5\frac{M_\odot}{L_{B,\odot}}}$$

In general: at least 5 times more dark matter then $M_{stars} + M_{\text{gas}}$!

5.9.2 Dark Matter concentrated in the Milky Way disk?

Historically important and first discussed by Oort in the thirties. Nowadays, the evidence is weak. The dark matter content of the Galactic disk is determined by the following procedure:

(1) count stars to determine the local luminosity density,
(2) measure the velocities of stars perpendicular to the disk to determine the velocity dispersion in z-direction,
(3) derive the mass density from the velocity dispersion using the Jeans equation for vertical equilibrium,
(4) compare local luminosity and mass density and check whether dark mass is needed.

In order to solve the Jeans equations, one generally makes a few simplifying assumptions:

(a) the radial dependencies and gradients are small compared to the ones in the z-direction.
(b) the disk is **isothermal** in in z-direction: $\sigma_z^2 := \overline{v_z^2} =$ const.

This is the simplest reasonable model for the vertical structure of spiral disks.

Relevant equations within the approximation:

$$\sigma_z^2 \frac{\partial \rho}{\partial z} = -\rho \frac{\partial \Phi}{\partial z} \qquad \text{Jeans equation in } z\text{-direction} \qquad (5.1)$$

$$\frac{\partial^2 \Phi}{\partial z^2} = 4\pi G \rho(z) \qquad \text{Poisson equation in } z\text{-direction} \qquad (5.2)$$

inserting (5.1) in (5.2):

$$-\frac{\partial}{\partial z}\left(\frac{\sigma_z^2}{\rho}\frac{\partial \rho}{\partial z}\right) = 4\pi G \rho \qquad (5.3)$$

Now substitute $\xi = \frac{z}{z_0}$ with:

$$z_0 = \sqrt{\frac{\sigma_z^2}{8\pi G \rho_0}} \tag{5.4}$$

and ρ_0 being a suitably chosen free factor. This yields:

$$\frac{\partial}{\partial \xi} \frac{1}{\rho} \frac{\partial \rho}{\partial \xi} = -\frac{\rho}{2\rho_0} \tag{5.5}$$

which has the following solution:

$$\boxed{\rho = \rho_0 \,\mathrm{sech}^2\left(\frac{\xi}{2}\right) = \rho_0 \,\mathrm{sech}^2\left(\frac{z}{2z_0}\right)} \qquad \text{with} \quad \mathrm{sech}(x) = \frac{2}{\exp(x) + \exp(-x)} \tag{5.6}$$

i.e. $\rho_0 = \rho(z = 0)$.

The derived density profile matches the observations in the optical.

This apparently confirms the assumption: $\sigma_z \sim$ const perpendicular to the equatorial plane. Equation (5.4) shows directly how the mass density in the disk is related to the scale height z_0 and the velocity dispersion σ_z. Therefore, by measuring σ_z and z_0 one can obtain ρ_0. Comparison with the density of stars and gas allows to conclude whether the disk contains dark matter or not. **The result is ambiguous at present.**

But:

- Due to dust absorption in the equatorial plane of spirals the optical determination of the vertical density profile is rather uncertain.
- Observations in the near IR (e.g. $\lambda = 2\mu m$) indicate, that the vertical density profiles of spiral disks are **probably closer to an exponential than an isothermal profile**:

$$\rho(z) = \rho_0 \exp\left(-\frac{z}{z_0}\right) \tag{5.7}$$

What are the properties of disks with vertically exponential profiles?

NGC 5907

courtesy: C. Gössl, Wendelstein Observatory, USM

σ_z profiles for disks with exponential z-profiles: $\rho(z) = \rho_0 e^{-z/z_0}$:

- First, we determine the potential from Poisson's equation:

$$\frac{\partial^2}{\partial z^2}\Phi_z = 4\pi G\rho(z)$$

which yields:

$$\Phi_z = 4\pi G\rho_0 z_0^2 \left(e^{-\frac{z}{z_0}} + c_1 z + c_0\right)$$

Since the acceleration in the equatorial plane must vanish, i.e. $\frac{\partial \Phi_z}{\partial z}\Big|_{z=0} = 0$, we conclude that $c_1 = \frac{1}{z_0}$. Furthermore, $c_0 = 0$ can be adopted. Thus:

$$\Phi_0(z) = 4\pi G\rho_0 z_0^2 \left(e^{-\frac{z}{z_0}} + \frac{z}{z_0}\right)$$

Note that in this way, for $z \gg z_0$, the asymptotic behaviour is identical to the one of the isothermal disk: $\Phi(z) \propto \frac{z}{z_0}$.

- The dynamics of the system can be determined from the Jeans equation:

$$\frac{1}{\rho}\frac{\partial}{\partial z}\left(\rho\sigma_z^2\right) = -\frac{\partial\Phi}{\partial z}$$

with the solution (exercise!):

$$\boxed{\sigma_z^2 = 4\pi G\rho_0 z_0^2\left(1-\frac{1}{2}e^{-\frac{z}{z_0}}\right)}$$

$\Rightarrow$ **vertically exponential disks are in the equatorial plane $\sim\sqrt{2}$ times cooler than in some scale heights distance from the equatorial plane**.

This is plausible! In the Milky Way we observe:

- young stars in the galactic disk are heavily concentrated around the equatorial plane and have relatively low velocity dispersions ($< 20\frac{\text{km}}{\text{s}}$), just like the gas (molecular clouds) they are formed from.
- older stars (like the sun) show higher dispersions ($\gtrsim 30\frac{\text{km}}{\text{s}}$) and are less concentrated around the equatorial plane. The likely reason is that the velocity dispersion of stars in the Milky Way grows with age due to scattering at molecular clouds, spiral arms etc.

$\Rightarrow$ The **galactic disk is cooler near the equatorial plane** (this can also be described by the superposition of several isothermal components).

5.9.3 Mass Determination of the Milky Way at Large Radii:

The mass of the Galaxy can be determined by measuring the distance and velocity of objects that are far away from the Galaxy (> 30 kpc), yet still gravitationally bound. Approximating the Galaxy as a point mass, these objects move on elliptical orbits with the Galaxy center in one of the focal points.

To describe the dynamics of the 'test particles', we use the spherical Jeans equation:

$$\frac{dn\overline{v_r^2}}{dr} + 2\beta n\frac{\overline{v_r^2}}{r} = -n\frac{d\Phi}{dr} = -n\frac{GM}{r^2}$$

where M is the mass of the Galaxy and $n(r)$ the radial density distribution of the test particles.

Multiplication with $4\pi r^4$ and integration yields:

$$\int_0^\infty \frac{dn\overline{v_r^2}}{dr} r^4 4\pi dr + \int_0^\infty 2\beta n\overline{v_r^2} r^3 4\pi dr = -GM\int_0^\infty n4\pi r^2 dr \qquad (5.8)$$

Partial integration of the first integral on the left side results in:

$$4\pi n\overline{v_r^2}r^4\Big|_0^\infty - \int_0^\infty 4n\overline{v_r^2}r4\pi r^2 dr$$

The first term vanishes for $r \to \infty$ because of $n = 0$ and at $r = 0$ because of r^4.

So for equation (5.8) follows:

$$\int_0^\infty \left(4n\overline{v_r^2}r - 2\beta n\overline{v_r^2}r\right) 4\pi r^2 dr = GM \int_0^\infty n4\pi r^2 dr$$

To simplify the problem we assume that β does not vary with radius:

$$(4 - 2\beta) \int_{-\infty}^{+\infty} \left(n\overline{v_r^2}r\right) d^3r = GM \int_{-\infty}^{+\infty} n d^3r$$

Now, we switch from a quasi continuous distribution of test particles to a finite number of objects via:

$$n = \sum_{i=1}^{N} \delta\left(\vec{r} - \vec{r_i}\right)$$

which yields:

$$(4 - 2\beta) \sum_{i=1}^{N} \left(v_r^2 r\right)_i = GMN$$

or:

$$\boxed{M = \frac{4 - 2\beta}{G} \left\langle v_r^2 r \right\rangle}$$

Lynden-Bell et al. (1983) used this equation to estimate the mass of the Galaxy from satellite galaxies or globular clusters (his paper had the title: 'Slippery evidence on the Galaxy's invisible heavy halo', *MNRAS*, **204**, 87).

Depending on the objects and the choice of β:

$$\boxed{M_{\text{Galaxy}} \simeq 0.2 \ldots 2 \cdot 10^{12} M_\odot}$$

(note that $L_{\text{Galaxy}} \simeq 2 \cdot 10^{10} L_{B,\odot}$).

Table 1 Determinations of Galactic mass as a function of galactocentric distance

R (kpc)	Method	Mass ($M_\odot$)	Reference
12–17	RR Lyraes toward the LMC (isotropic velocities)	$2.6–2.9 \times 10^{11}$	148
17	Globular cluster velocities	2×10^{11}	106
20	Globular clusters (circular orbits)	$0.3–0.8 \times 10^{11}$	487
	(isotropic orbits)	2×10^{11}	
44	Globular cluster and satellite galaxy tidal radii	$8.9 \pm 2.6 \times 10^{11}$	333
50	Halo star and cluster velocities	4.4×10^{11}	489
65	Escape velocity of 3 RR Lyraes	$10–30 \times 10^{11}$	282
50–100	Globular clusters (isotropic velocities)	$5 \pm 2 \times 10^{11}$	497
	(no radial orbits)	10×10^{11}	
50–100	Globular cluster velocities	2×10^{11}	676
100	Globular cluster and satellite velocities (if all bound)	9×10^{11}	471
100	Globular cluster isotropic velocities	10×10^{11}	523
118	One globular cluster	$\leq 10 \times 10^{11}$	654
Total	Escape velocities of field halo stars	$\geq 5 \times$ mass to R_0	125
Total	Globular cluster and satellite galaxy tidal radii	10×10^{11}	138

see: Trimble V. (1987) *ARAA*, **25**, 425

5.10 The Orbits of Stars in Disks: The Epicycle Approximation

In the disks of spiral or S0 galaxies many stars are on nearly circular orbits. Therefore, to describe their dynamics, it is sufficient to derive approximate solutions based on perturbed circular orbits.

We define variables x, θ describing the deviations of the coordinates of the stars from their coordinates on a circular orbit, i.e.

$$x(t) \equiv r(t) - R, \tag{5.9}$$

$$\theta(t) \equiv \varphi(t) - \Omega t, \tag{5.10}$$

where R and Ω are the radius and angular velocity of a star on a circular orbit.

The solution for the circular orbit yields

$$\left(\frac{\partial \Phi}{\partial R}\right)_{(R,0)} = \frac{v_{circ}^2}{R} = \Omega^2 R \tag{5.11}$$

with the circular velocity v_{circ}.

The Newtonian equations of motion in cylindrical coordinates read:

$$\ddot{r} - \dot{\varphi}^2 r = -\frac{\partial \Phi}{\partial r}, \tag{5.12}$$

$$r\ddot{\varphi} + 2\dot{r}\dot{\varphi} = 0, \tag{5.13}$$

$$\ddot{z} = -\frac{\partial \Phi}{\partial z}. \tag{5.14}$$

Expanding the potential Φ in a Taylor series about $(R, 0)$ yields:

$$\frac{\partial \Phi}{\partial r} = \frac{\partial \Phi}{\partial r}(R,0) + x\frac{\partial^2 \Phi}{\partial r^2}(R,0) + \mathcal{O}\left(x^2, \theta^2, z^2\right) \tag{5.15}$$

[Remark: All other terms vanish because of

$$\left(\frac{\partial^2 \Phi}{\partial r \partial \varphi}\right) = 0 \quad \text{due to} \quad \left(\frac{\partial \Phi}{\partial \varphi}\right)_{(R,0)} = 0 \tag{5.16}$$

$$\left(\frac{\partial^2 \Phi}{\partial r \partial z}\right) = 0 \quad \text{due to} \quad \left(\frac{\partial \Phi}{\partial z}\right)_{(R,0)} = 0 \tag{5.17}$$

(axisymmetry and symmetry about $z = 0$).]

The equations of motion then have the following form:

$$\ddot{x} \; - \; 2\,\Omega\,\dot{\theta}\,R \; - \; \Omega^2\,x \; = \; -x\left(\frac{\partial^2\Phi}{\partial r^2}\right)_{(R,0)} \tag{5.18}$$

$$R\,\ddot{\theta} \; + 2\,\dot{x}\,\Omega \; = \; 0 \tag{5.19}$$

$$\ddot{z} \; = \; -z\left(\frac{\partial^2\Phi}{\partial z^2}\right)_{(R,0)} \tag{5.20}$$

This approximation of the equations of motion is called **epicycle approximation**.

The second of the epicycle equations has the solution

$$R\,\dot{\theta} \; + \; 2\,x\,\Omega \; = \; \text{const.} \; \stackrel{!}{=} \; 0 \tag{5.21}$$

(without loss of generality we can choose the constant to be zero).

With this solution the first epicycle equation can be rewritten as

$$\ddot{x} \; = \; -\left[\left(\frac{\partial^2\Phi}{\partial r^2}\right)_{(R,0)} \; + \; 3\,\Omega^2\right]\,x \; \equiv \; -\,\kappa^2\,x \tag{5.22}$$

which is the equation of motion for the **harmonic oscillator**.

Using

$$\left(\frac{\partial \Phi}{\partial r}\right)_{(R,0)} = \Omega^2 r \tag{5.23}$$

and

$$\left(\frac{\partial^2 \Phi}{\partial r^2}\right)_{(R,0)} = \Omega^2 + r \left(\frac{\partial \Omega^2}{\partial r}\right)_{(R,0)} \tag{5.24}$$

we find

$$\boxed{\begin{aligned} \ddot{x} &= -\kappa^2 x, \\ \kappa^2 &= R\,\tfrac{d\Omega^2}{dR} + 4\,\Omega^2 \end{aligned}}$$

which simply shows that in our approximation the star performs radial oscillations with frequency κ around the circular orbit.

What is a plausible range of values for κ?

To answer this question, let us investigate some special cases:

1. Limit: Rotation of a rigid body (i.e. $\Omega(R) = \text{const.}$), which is the rotational behaviour we observe for the central regions of galaxies. In this case we find

$$\kappa = 2\Omega$$

2. Limit: Constant rotational velocity (i.e. $\Omega(R) \propto R^{-1}$), for which the definition of κ yields

$$\kappa = \sqrt{2}\Omega$$

3. Limit: Keplerian rotation (i.e. $\Omega(R) \propto R^{-3/2}$) which is the steepest decrease possible. Then:

$$\kappa = \Omega$$

Thus in almost all cases:

$$\boxed{\Omega \leq \kappa \leq 2\Omega}$$

This means that stars oscillate only slowly around the circular orbit. The orbits are generally not closed.

Interesting consequences arise if the disk is not fully axisymmetric. E.g., assume that the potential is disturbed by spiral structure or a bar which rotates with a pattern speed Ω_p and corresponds to typically a 10% disturbance in mass or potential. Then resonances can occur. If for integer m

$$m(\Omega - \Omega_p) = \pm\kappa$$

then the star encounters successive crests of the potential at a frequency which coincides with the frequency of its natural radial oscillations (see Binney & Tremaine, Galactic Dynamics). The resonances are named after the Swedish astronomer Bertil Lindblad and occur at the so-called **Lindblad radii**. They play an important role in the study of bars and spiral structure.

5.11 Stability of Disks

Disks are relatively fragile objects. Generally, disks with a higher velocity dispersion are more stable against perturbations. From dynamical analysis, Toomre (1964) obtained the following criterion:

Disks are stable if:

$$\boxed{Q \equiv \frac{\sigma_r}{3.4\frac{G\Sigma(r)}{\kappa}} > 1} \qquad \text{Toomre's } Q \text{ parameter}$$

with the mass surface density $\Sigma(r)$, the epicycle frequency κ and the radial dispersion σ_r

Example: Galactic disk in solar neighborhood:

$$\left.\begin{array}{l} \Sigma(R_\odot) \simeq 80 \pm 10 \ \frac{M_\odot}{\text{pc}^2} \\ \kappa \simeq 35 \ \frac{\text{km}}{\text{s kpc}} \\ \sigma_r \simeq 40 \ \frac{\text{km}}{\text{s}} \end{array}\right\} \quad Q_\odot \simeq 1.2 \quad \rightsquigarrow \text{marginally stable}$$

If $Q < 1$: the disk is unstable: $\Rightarrow$ **formation of bars** ...

5.12 Spiral Structure in Disks

- Spiral arms cannot rotate with the local circular velocity in the disk, because then they would wind up. (The revolution time is much shorter at small radii than at large ones: Ω is not constant, in general: $\Omega \propto 1/r$)

- $\Rightarrow$ Spiral arms are made up of **different stars at different times**!
  $\Rightarrow$ Spiral arms are a **wave phenomenon**!

  This can be described in a plausible way by the density wave theory.
  (Lindblad (1963), Lin & Shu (1964-70))

  Hypothesis: The spiral structure is a stationary or quasi-stationary phenomenon.

- The density wave theory cannot always provide a satisfactory description, especially in the case of **"stochastic" spirals**, e.g. NGC2841. Self-propagating star formation and differential rotation can result in a structure similar to spiral arms.

- Bars seem to favour the formation of spiral arms.

- Very prominent spiral arms seem to form in interacting spiral galaxies (M51, M81). The interaction can trigger the density wave or amplify it.

NGC 2841

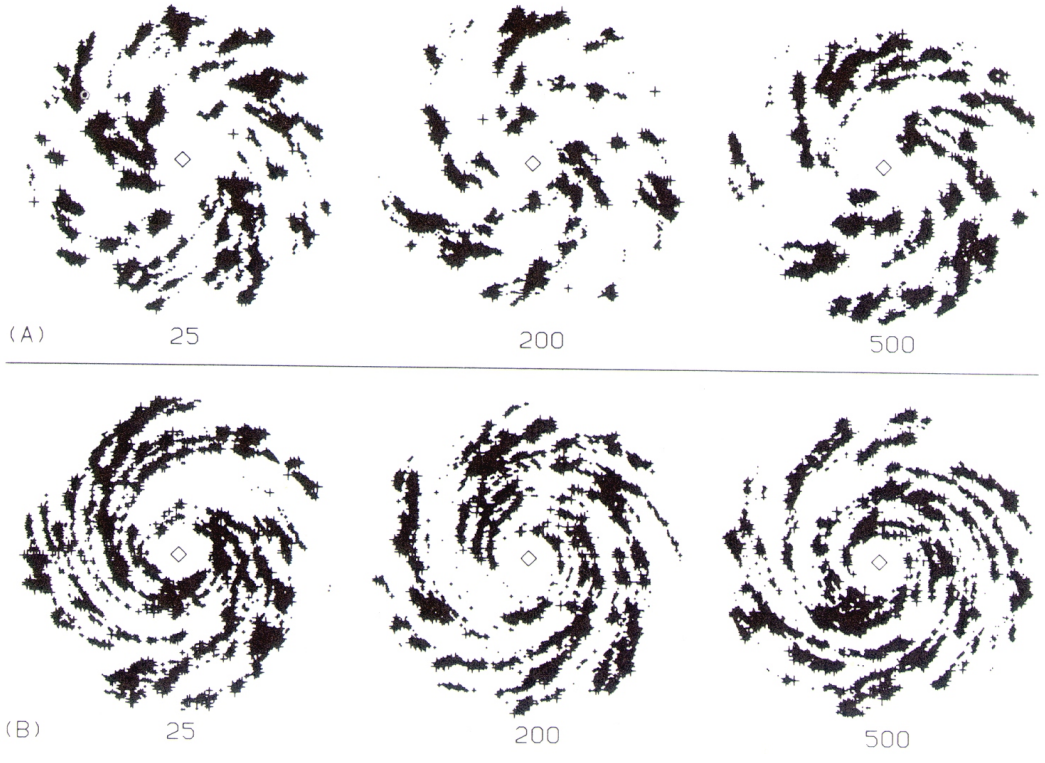

Numerical simulations of stochastic self-propagating star formation in spirals (Gerola & Seiden (1978) *ApJ*, **223**, 129). Numbers give the time in units of 15 Mio. years, the upper panel is for the rotation curve of M101, the lower for M81.

courtesy: C. Gössl, Wendelstein Observatory, USM

Interacting spiral galaxy M51

5.12.1 Spiral Structure and Star Formation

Spiral structure and star formation are closely linked via the following sequence of events:

$\rightarrow$ the spiral density wave compresses the gas in the disk (which enhances the strength of the density wave)
$\rightarrow$ molecular clouds collide and collapse
$\rightarrow$ star formation sets in

Spiral arms are very prominent in the blue light and the H_α line, because of the short-lived massive blue stars forming in the wake of the density wave.

5.13 Simulations of the Spiral Structure

5.13.1 Spontaneous Spiral Structure

Swing amplification of particle noise can bring forth trailing **multi-armed** spiral patterns. Shown here is an N-body experiment with a central bulge (yellow), an exponential disk (blue), and a dark halo (red). Apart from Poissonian fluctuations due to particle noise, this disk is initially featureless. Later frames, separated by about half a rotation period at three exponential scale lengths, show the development of transient spiral patterns.

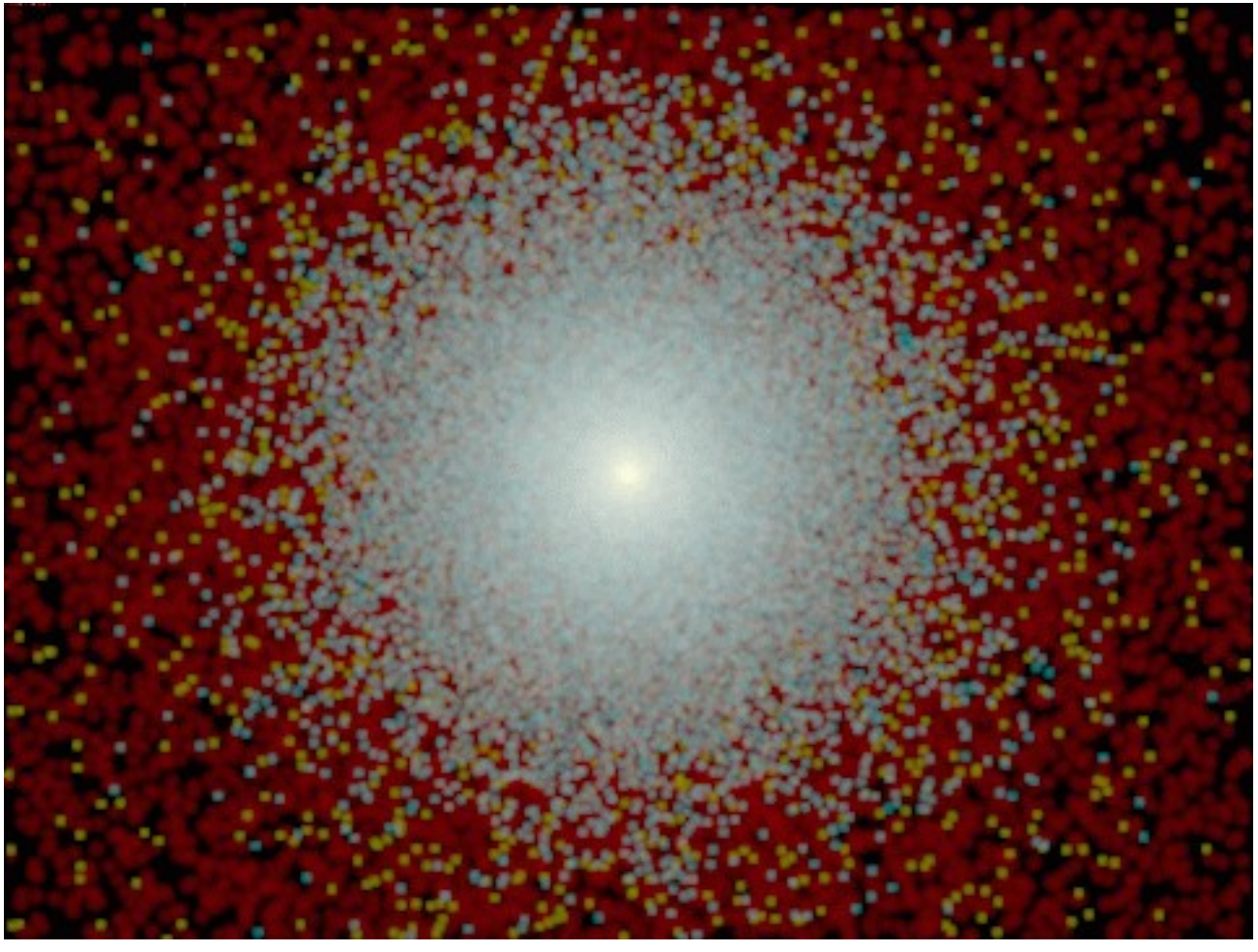

see: Barnes, J. E.: Institute for Astronomy, University of Hawaii

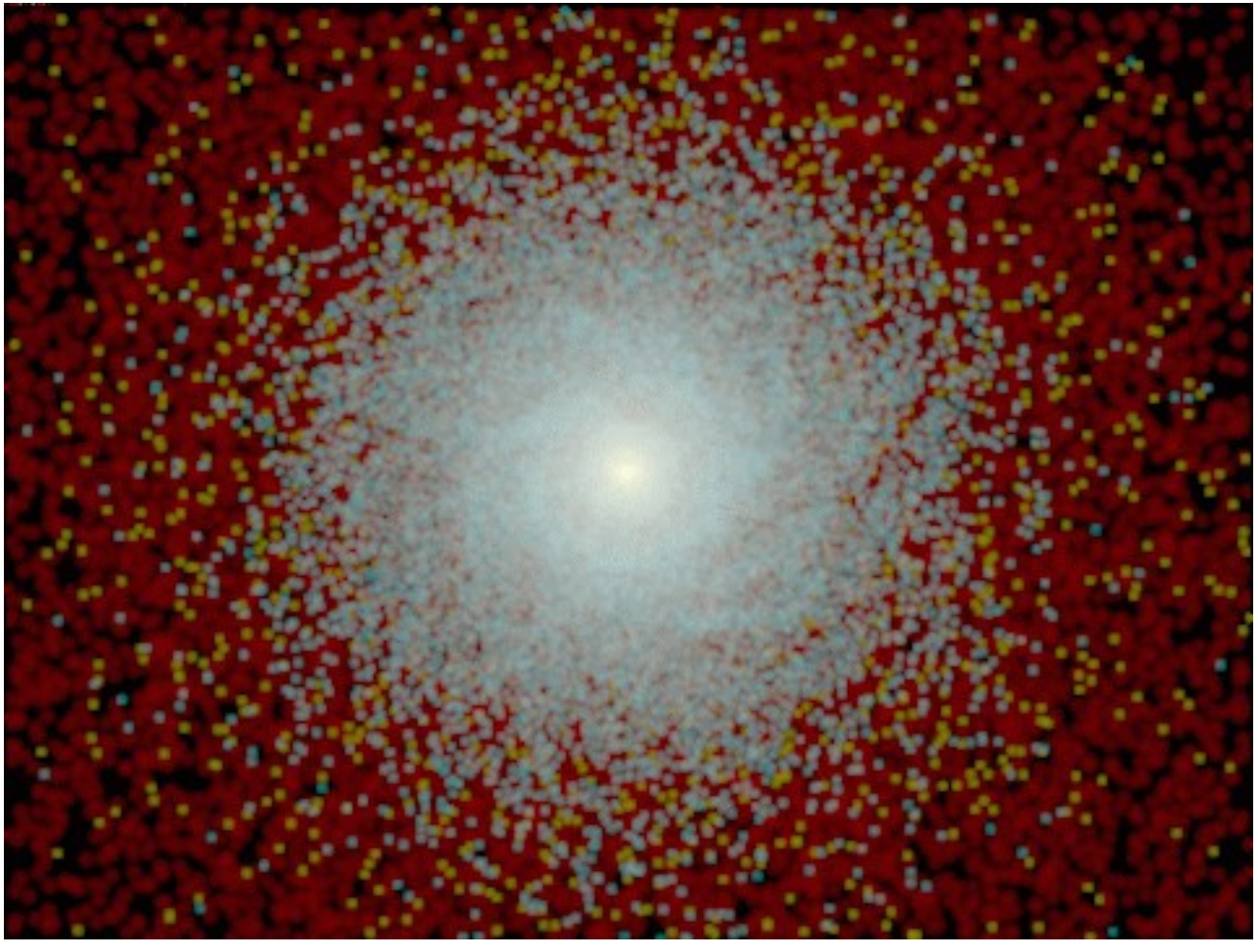

see: Barnes, J. E.: Institute for Astronomy, University of Hawaii

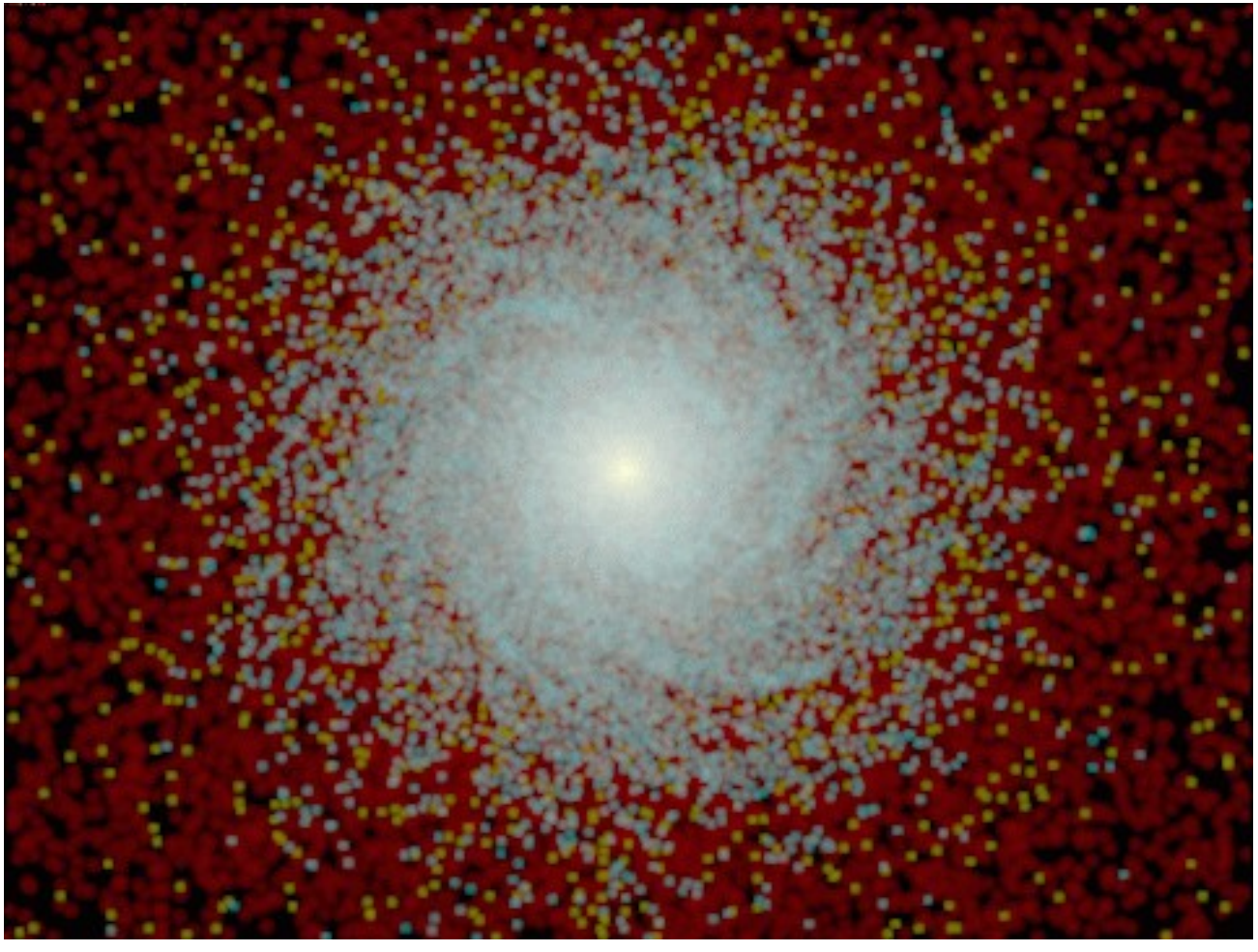

see: Barnes, J. E.: Institute for Astronomy, University of Hawaii

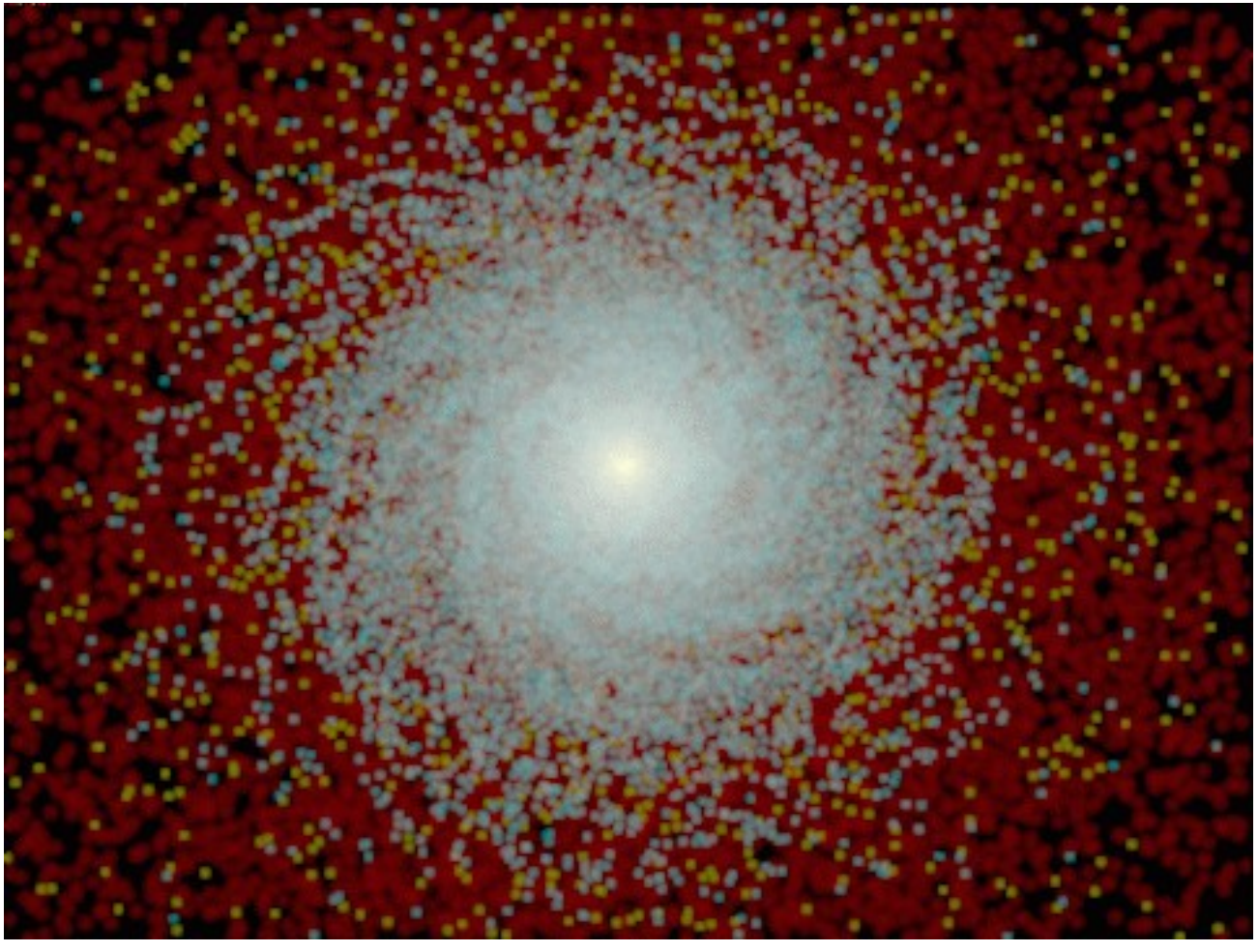

see: Barnes, J. E.: Institute for Astronomy, University of Hawaii

5.13.2 Tidal Spiral Structure

Tides between galaxies provoke a two-sided response. Such perturbations, if further swing-amplified in differentially-rotating disks, may produce striking ‘grand-design’ spiral patterns. In the experiment shown here, an artificial tide was applied by taking the unperturbed disk above and instantaneously replacing each x velocity with

$$v_x \leftarrow v_x + kx$$

where k is a constant used to adjust the strength of the perturbation. No perturbation was applied to the y and z velocities. Frames made after 1.5 rotation periods show the development of an open, **two-armed** spiral pattern which becomes more tightly wound with time.

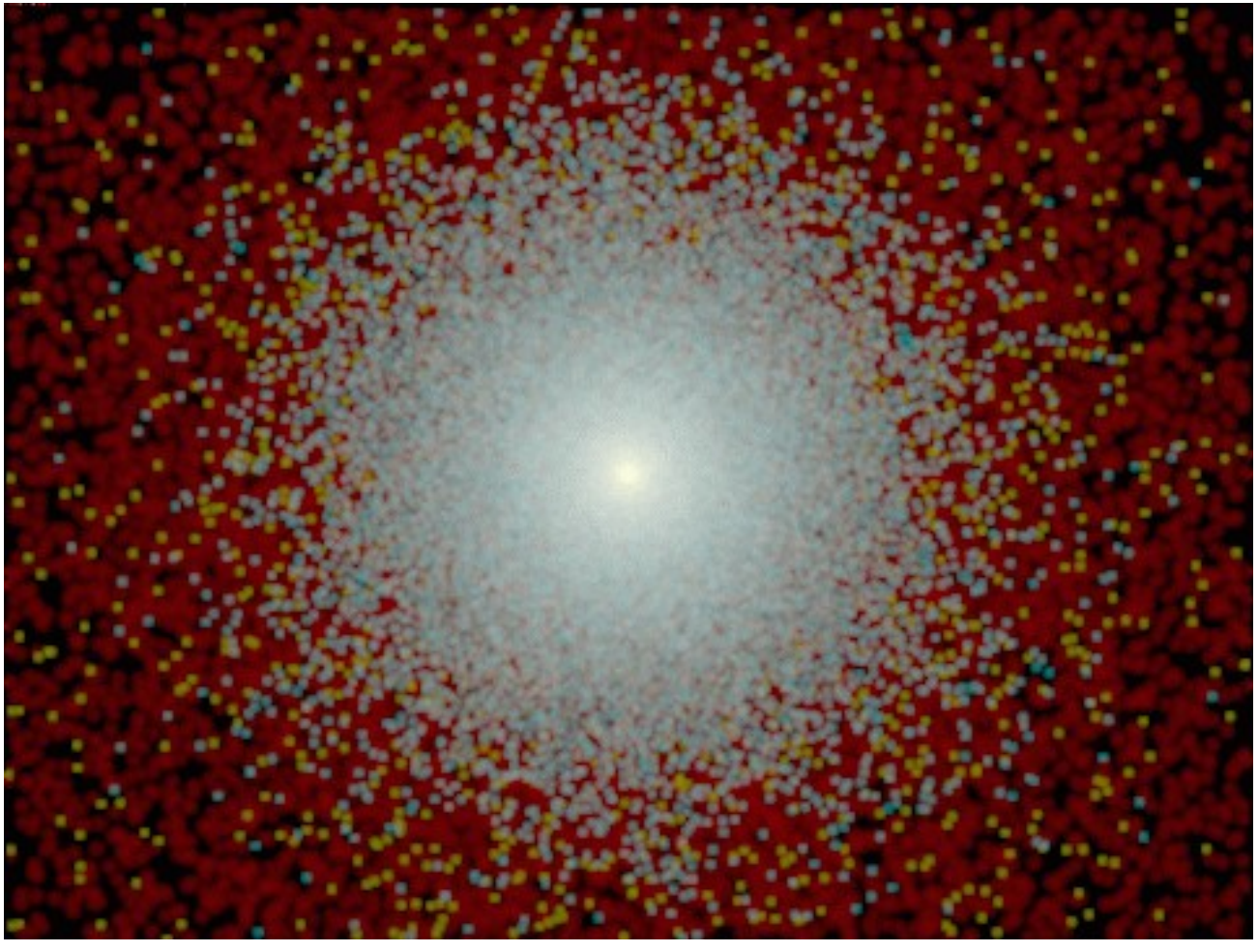

see: Barnes, J. E.: Institute for Astronomy, University of Hawaii

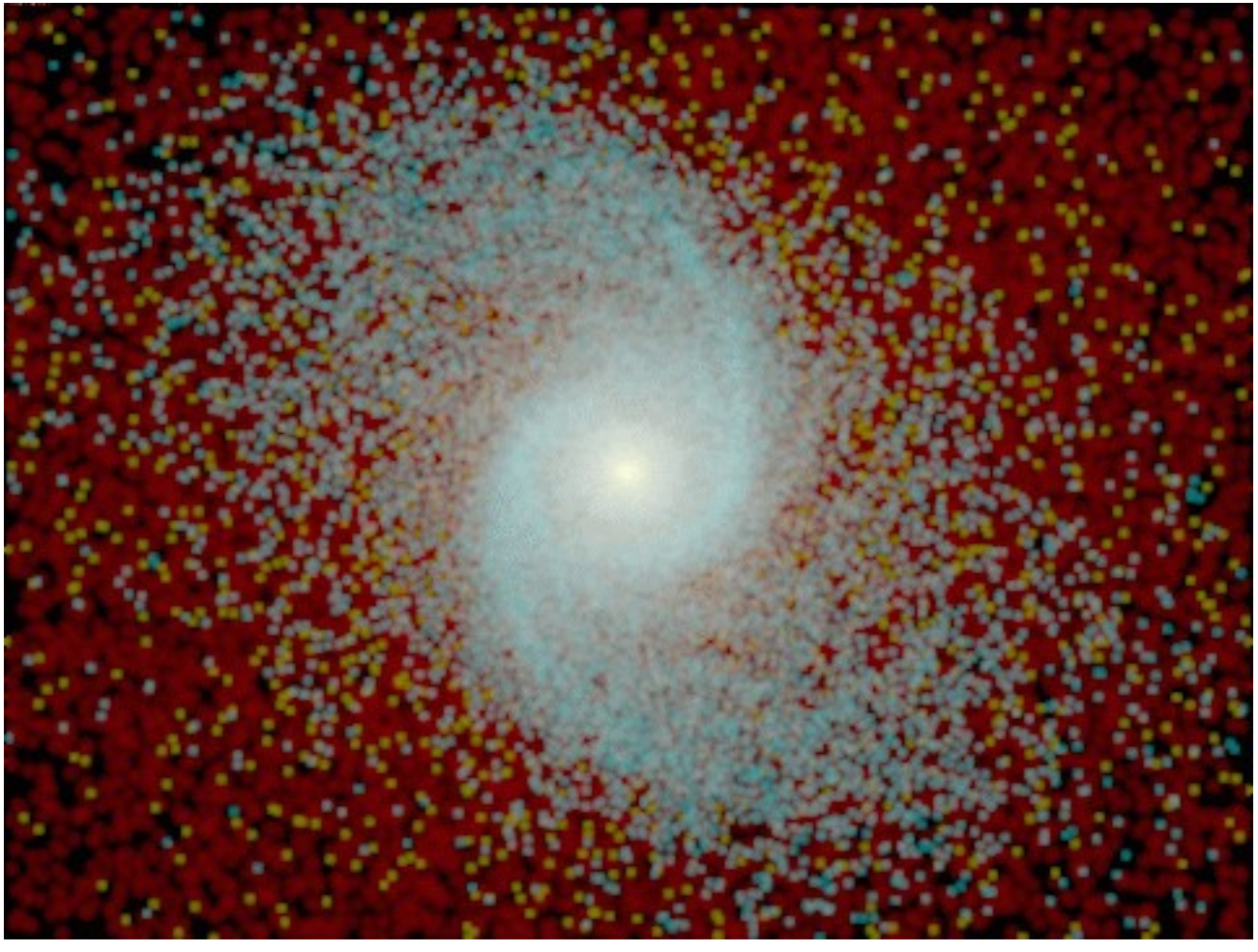

see: Barnes, J. E.: Institute for Astronomy, University of Hawaii

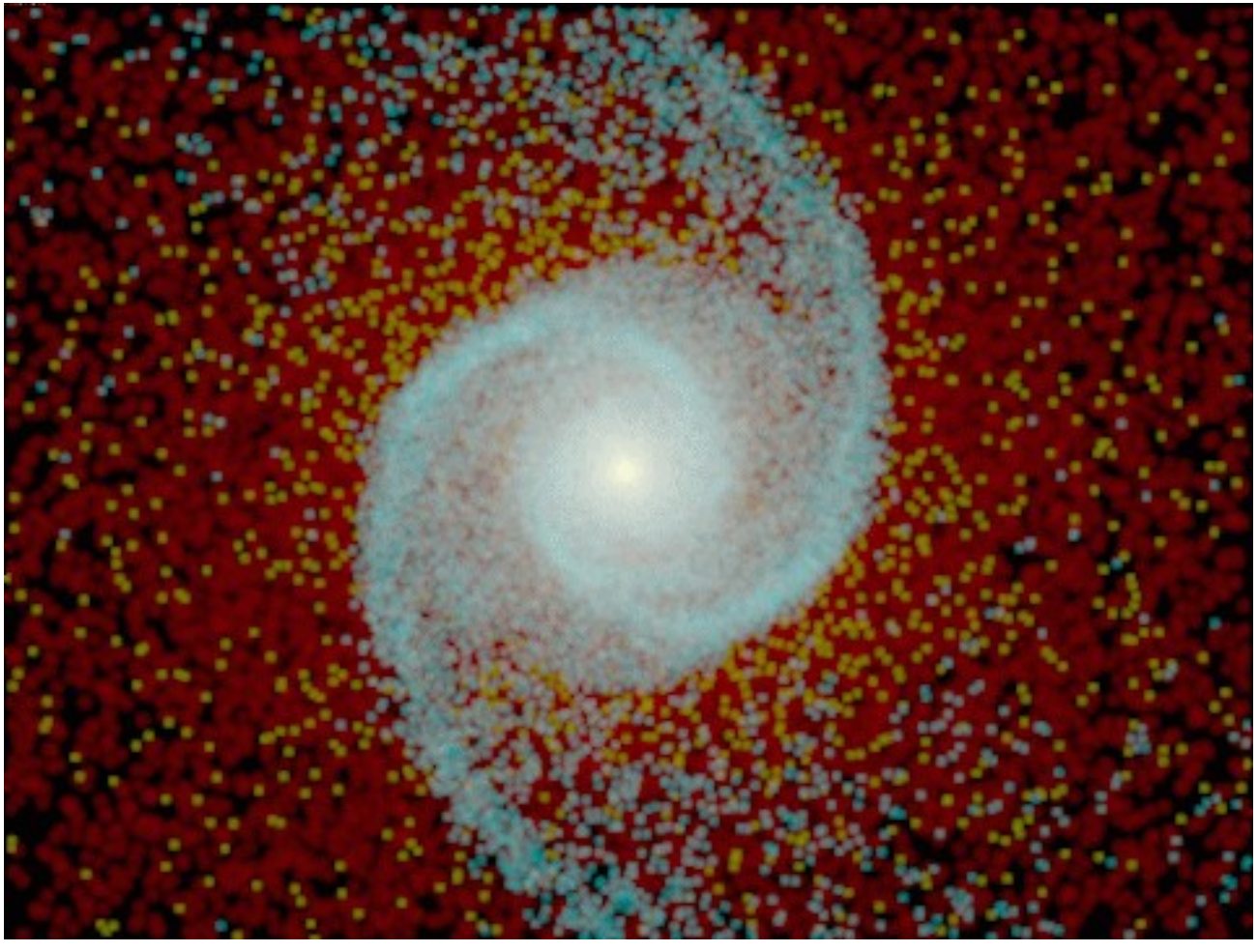

see: Barnes, J. E.: Institute for Astronomy, University of Hawaii

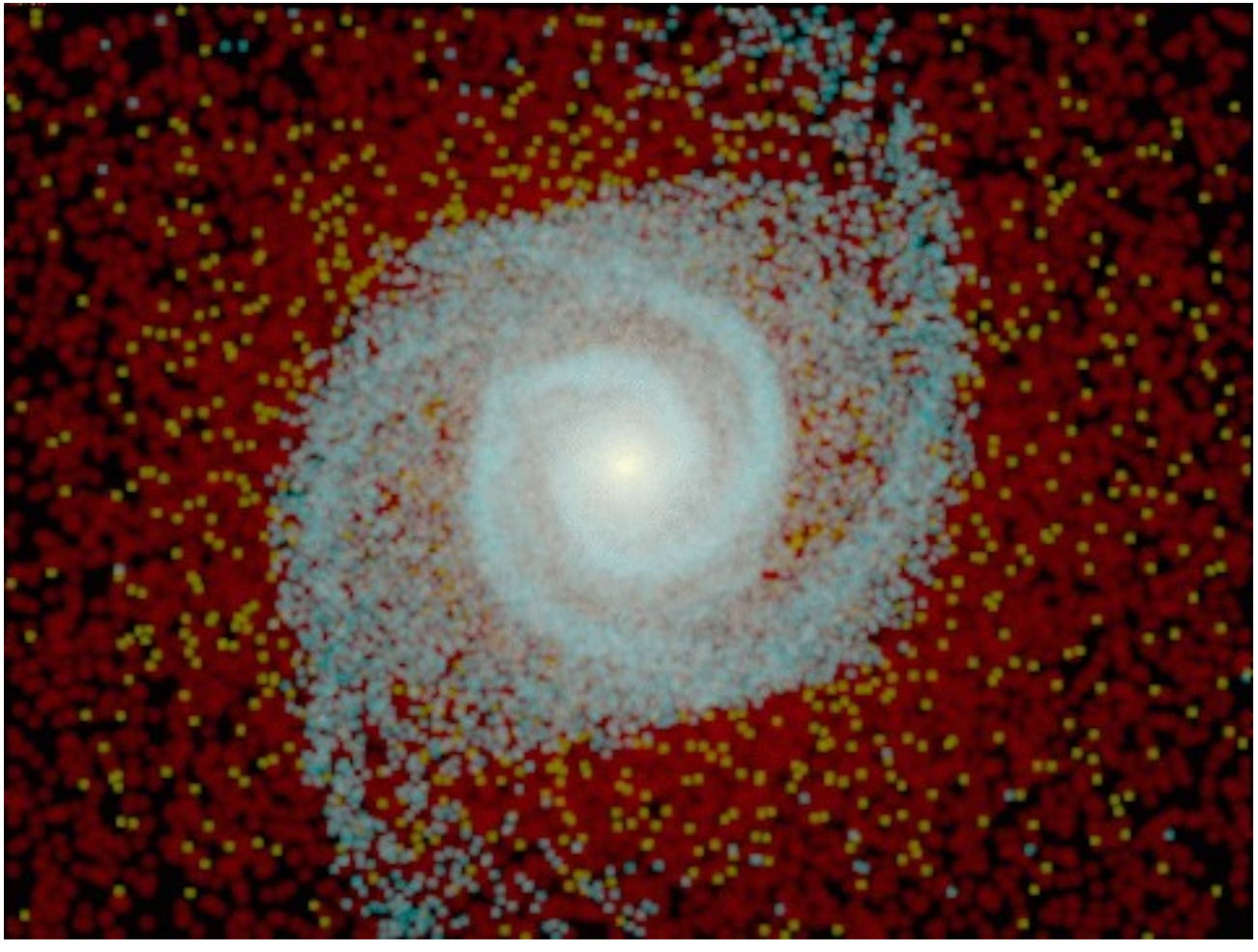

see: Barnes, J. E.: Institute for Astronomy, University of Hawaii